IEEE Access
Multidisciplinary ⋮ Rapid Review ⋮ Open Access Journal

Received June 10, 2020, accepted July 9, 2020, date of publication July 17, 2020, date of current version August 5, 2020.

Digital Object Identifier 10.1109/ACCESS.2020.3009898

Optimized Edge Detection Technique for Brain Tumor Detection in MR Images

AHMED H. ABDEL-GAWAD[1], LOBNA A. SAID[1], (Senior Member, IEEE), AND AHMED G. RADWAN[2,3], (Senior Member, IEEE)

[1]Nanoelectronics Integrated Systems Center, Nile University, Giza 12588, Egypt
[2]Department of Engineering Mathematics and Physics, Cairo University, Giza 12613, Egypt
[3]School of Engineering and Applied Sciences (EAS), Nile University, Giza 12588, Egypt

Corresponding author: Lobna A. Said (l.a.said@ieee.org)

This work was supported by the Egyptian Science and Technology Development Fund (STDF) under Project 25977.

ABSTRACT Genetic algorithms (GAs) are intended to look for the optimum solution by eliminating the gene strings with the worst fitness. Hence, this paper proposes an optimized edge detection technique based on a genetic algorithm. A training dataset that consists of simple images and their corresponding optimal edge features is employed to obtain the optimum filter coefficients along with the optimum thresholding algorithm. Qualitative and quantitative performance analyses are investigated based on several well-known metrics. The performance of the proposed genetic algorithm-based cost minimization technique is compared to the classical edge detection techniques, fractional-order edge detection filters, and threshold-optimized fractional-order filters. As an application for the proposed algorithm, a strategy to detect the edges of the brain tumour from a patient's MR scan image of the brain is proposed. First, Balance Contrast Enhancement Technique (BCET) is applied to improve the image features to provide better characteristics of medical images. Then the proposed GA edge detection method is employed, with the appropriate training dataset, to detect the fine edges. A comparative analysis is performed on the number of MR scan images as well. The study indicates that the proposed GA edge detection method performs well compared to both classical and fractional-order edge detection methods.

INDEX TERMS Edge detection, optimization, genetic algorithm, image processing, medical imaging, tumor detection.

I. INTRODUCTION

The early stage of visual processing is to identify features in images that are relevant to estimating the structure and properties of objects in a scene; edges are one such feature. Edges are significant local changes in the image intensity, usually associated with a discontinuity in either the image intensity or the first derivative of the image intensity, and both are important features for analyzing images. Edge detection is essentially a series of mathematical methods that identify those changes. Edge detection is frequently the first step in recovering information from images.

Many gradient-based edge detectors have been developed in the last two decades. Roberts cross operator is one of the first edge detectors [1] that computes quickly and simply the 2D spatial gradient measurement on an image. It, thus, highlights regions of high spatial frequency which often correspond to edges. The Prewitt operator uses two kernels which are convolved with the original image to calculate an approximation of the derivatives for horizontal and vertical change [2]. The Sobel operator is a discrete differentiation operator that computes an approximation of the gradient of the image intensity function [3], [4].

The associate editor coordinating the review of this manuscript and approving it for publication was Yan-Jun Liu.

A. CLASSICAL EDGE DETECTORS

The Laplacian-based edge detectors find image edges by computing the second-order derivative expression of the image. The second-order expression has zero-crossing where the image edges are found. Edge points detected by finding the zero-crossing of the second derivative of the image intensity are very sensitive to noise. Therefore, Laplacian of Gaussian (LoG) combines Gaussian filtering with the Laplacian for edge detection to filter out the noise [5].

There is a trade-off between noise suppression and localization. The type of linear operator that provides the best

compromise between noise immunity and localization, while retaining the advantages of Gaussian filtering, is the first derivative of a Gaussian [6].

The canny edge detector is the first derivative of a Gaussian and it closely approximates the operator that optimizes the product signal-to-noise ratio and localization [7]. The Canny edge detection algorithm runs mainly in four sequential steps; smooth the image with a Gaussian filter, compute the gradient magnitude and orientation using finite-difference approximations for the partial derivatives, apply non-maxima suppression to the gradient magnitude, and use the double thresholding algorithm to detect and link edges [8].

B. FRACTIONAL-ORDER EDGE DETECTORS

Fractional calculus, also called non-integer order calculus, is a generalization of the conventional calculus. The concept of fractional calculus appeared in the same era with the traditional calculus in the early nineteenth century. Due to the efforts of many scientists, in the past two hundred years, fractional calculus has developed to be a standalone pure mathematical branch [9]–[12]. It caught the attention of scientists and engineers to be applied in many applications of various fields [13]–[18]. This paper is focusing on its use in the image processing field [19], [20]. In image processing, it was found that the fractional differential operators have many advantages over the integer-order ones. The fractional derivative involves an infinite number of terms, unlike the integer derivative which includes finite terms. Thus, the fractional derivative is considered to be a global operator. The fractional operator considers more neighbouring pixels information, extracting more image texture details.

There exist different definitions of the fractional-order differentiation; the very well-known definitions are the Riemann-Liouville's definition and the Caputo's definition [10]. However, the Grunwald-Letnikov's (G-L) definition is easier to be applied in numerical analysis. Most of the classical edge detection algorithms mainly use integer-order filters, namely the first-order derivative of the gradient operator or the second-order derivative of the Laplacian operator. The first-order derivative methods generally produce thicker edges, which may result in the loss of some image details. On the other hand, the second-order derivative methods are more reliable in detecting fine detail, but they are more noise sensitive. This conflict can be crucially solved using fractional-order derivatives.

Some work was introduced using fractional-order operators in image edge detection [21]. In [22], a generalization of the first-order Sobel operator was proposed, which employed the frequency characteristic of the fractional derivative for extracting more structure feature details in medical images. In an attempt to resolve some noise issues, an operator [23] based on fractional calculus with improved characteristics over the classical methods was proposed. Improved covering templates of the fractional differential on x and y coordinates by using the G-L definition of fractional calculus, a generalized fractional-order filter, was presented in [24]. A study was done in [25], which proposed the combination of fractional-order edge detection (FOED) and a chaos synchronization classifier for fingerprint identification. An algorithm based on the fractional difference was used for the edge extraction of the palm print image in [26]. Three filter templates were constructed in [26] to extract the palm print edge. One of them is chosen for the comparative study of this paper.

C. EVOLUTIONARY ALGORITHMS

Evolutionary algorithms such as genetic algorithm-based cost optimization [27]–[29] were applied for edge detection to overcome the drawbacks of classical approaches. However, it is still a significant challenge in image processing to get the optimal threshold for each image, as these traditional techniques have limitations of using the fixed value of thresholds [30]. Soft computing as compared to the traditional techniques can deal with the mystery and uncertainty in image processing in a better way. It can build a machine that can work as a human to develop intelligence [31]. Optimization of different edge detection techniques has been applied to prove that it's applicable. A fully automatic way to cluster an image using the K-means principle has been applied in [32] to extract the required number of thresholds where a genetic algorithm was used to choose the optimum threshold levels for each image.

D. TUMOR DETECTION

Image processing techniques play an essential role in the diagnosis of diseases and monitoring patients. Edge detection is a fundamental task in image processing, particularly in the areas of feature detection and feature extraction directed at the search of identifying points, in which the image has discontinuities [33]. For the detection of tumours, Computed Tomography (CT) or Magnetic Resonance Imaging (MRI) are used. Corresponding medical equipment of these types brings a noticeable fraction of noise in the obtained images [34]. Therefore, noise suppression [35], [36] is a necessary step to improve the accuracy of image analysis.

The existing methods of tumor detection [37]–[39] and evaluation are divided into region-based and contour-based methods. Region-based methods [40]–[43] seek out clusters of pixels that share some measure of similarity. These methods include low-level operations, such as threshold selection, histogram analysis, classification, etc. In general, these methods take advantage of only local information for each pixel and do not include the shape and the boundary information. Contour-based methods [44]–[46] rely on the evolution of a curve based on the internal and external forces, such as image gradient, to delineate the boundary of brain structure or pathology. Many researchers use a wide range of techniques based on segmentation to solve the problem of localizing and analyzing the characteristics of a brain tumour. In [47], medical image segmentation based on morphological operators was conducted along with threshold selection. In [48], morphological operations were used along with threshold

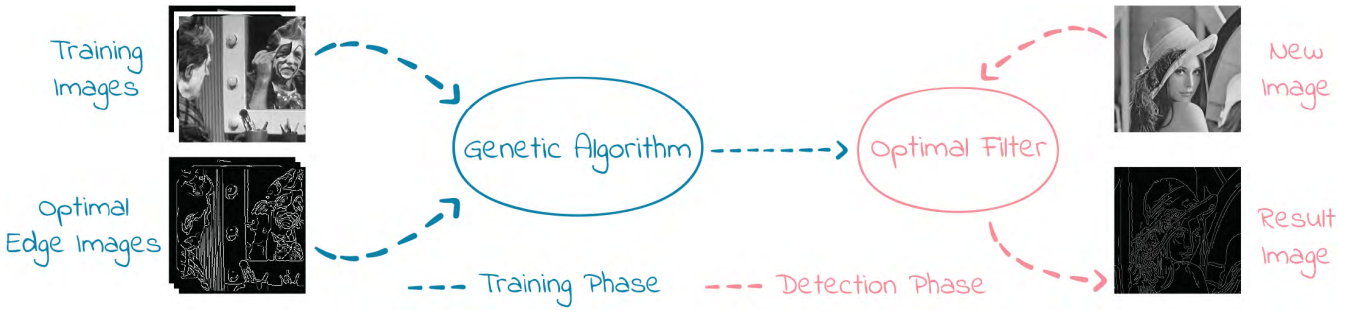

FIGURE 1. The Proposed GA Edge Detection method.

and watershed segmentation. Also, FCM clustering method is often used for image segmentation [44], [45].

In this paper, a new method of edge detection is proposed, which employs a Genetic Algorithm (GA) to optimize the filter coefficients and choose the optimum thresholding algorithm. The proposed method block diagram is represented in Figure 1. The algorithm takes a group of training images, which consists of simple images and its corresponding optimal edge features, as input, and starts optimizing the coefficients of the filter using the genetic algorithm as demonstrated in section II. The output trained filter is then tested to new images to detect edges. Alongside the kernel coefficients, there exist other factors that also affect the edge detector performance and can be optimized using the GA. One such factor is the thresholding algorithm. The paper also introduces an application of the proposed Edge Detection method for detecting brain tumours in MR scan images. The proposed method is applied to the Region of Interest (ROI), e.g. the region which has a tumour, to detect the tumour edges after performing some image enhancement operations including skull stripping and Balance Contrast Enhancement Technique (BCET).

The rest of the paper is organized as follows: Section II gives descriptions of the proposed edge detection method. Section III presents the performance measures for evaluating the proposed edge detection method. The results are presented and analyzed in Section IV. Section V describes the use of the proposed edge detection method in brain tumour detection. Finally, the whole work is concluded in Section VI.

II. PROPOSED EDGE DETECTION METHOD

Genetic algorithms (GAs) [49] are biologically inspired techniques which represent a new computational model having its roots in evolutionary sciences. Usually, GAs describe an optimization procedure in a binary search space. They do not evaluate and improve a single solution, but a set of solutions or hypotheses, a so-called population. The GAs produce successor hypotheses by mutation and recombination of the best currently known hypotheses. Thus, at each iteration, a part of the current population is replaced by the offspring of the fittest hypotheses. In other words, a space of candidate hypotheses is searched to identify the best hypothesis, which is defined as the optimization of a given numerical measure, the so-called hypothesis fitness [50]. A fitness function is used to evaluate the performance of chromosomes in the population. The fitness function takes a chromosome as input and returns a number which is a measure of the chromosome's performance. The fitness value determines the probability that a given chromosome will survive and be selected for reproduction in the succeeding generation(s).

Finding a fitness function is the hardest part when it comes to formulating a problem using genetic algorithms. The fitness function gives, based on the measured performance, the chance of reproductive opportunities. In other words, it defines the criterion for ranking potential hypotheses and for probabilistically selecting them for inclusion in the population of the next generation.

An underlying genetic algorithm training system is employed to optimize the coefficients of the edge detection filter, a thresholding algorithm, as demonstrated in Algorithm 1.

Genetic Algorithm (GA) begins with a set of k randomly generated individuals called 'population'. Each individual is represented by a one-dimensional string. This string is called 'chromosome' with each symbol named 'gene'. GA then uses iterative methods to produce a new population. The basic steps of GA are as follows [51]:

- **Selection**: The selection is aimed to pick the fittest individuals from the present population and give them the chance to be the descendants of the next generation. The individuals selected are then grouped into pairs.
- **Crossover**: Through the crossover operation, another generation of individuals can be obtained, which combines the parent's features. The algorithm chooses one-cut point randomly, then recombines two parent's right parts with probability P_c to produce an offspring.
- **Mutation**: An individual is randomly selected, then each 'gene' in the selected individual is randomly mutated with a certain probability of P_m

For canonical GAs, the definition of the fitness function is given by $f_i/\bar{f}$, where f_i is the evaluation associated with chromosome i and $\bar{f}$ is the average evaluation of all strings in the population. $\bar{f}$ is given by Equation 1. Apart from these very simple operations, many others have been proposed in

Algorithm 1 Classic Genetic Algorithm

1: Initialize population randomly for the strings a_i $\Pi = \{a_i\}, i = 1, 2, \ldots, n$
2: **while** $i <$ *Numberofgenerations* **do**
   Initialize mating set $M \leftarrow \varnothing$ and Offspring O
3: **while** $i < n$ **do**
   Add $f_i/\bar{f}$ copies from a_i to M
4: **end while**
5: **while** $j < \frac{n}{2}$ **do**
   Choose two parents a_j and a_k from M and perform with probability P_c $O = O \cup Crossover(a_j, a_k)$
6: **end while**
7: **while** $i < n$ & $j < n$ **do**
   Mutate with the probability P_m the j^{th} bit from $a_i \in O$ Update the population $\Pi \leftarrow combine(\Pi, O)$
8: **end while**
9: **end while**

the literature [52].

$$\bar{f} = \frac{1}{n}\sum_{i=1}^{n} f_i. \tag{1}$$

A. GENETIC EDGE EETECTOR

There exist two major requirements that need to be met so that a GA can solve a given problem. First, the problem must have a genetic representation capability. This requires that the values and variables are capable of being stored and mutated in a meaningful way. Second, a fitness function must exist so that each solution can be graded to enable optimal results to be selected.

1) GENETIC REPRESENTATION OF EDGE DETECTION PROBLEM

Any edge detection method can be represented as two operation filters. A one-dimensional number array can be made directly from these filters. Equation 2 shows the genetic representation of the x-direction filter of the Sobel operator. As one filter can be expressed as a transform of the other, only one should be considered.

$$S_x = \begin{bmatrix} -1 & 0 & +1 \\ -2 & 0 & +2 \\ -1 & 0 & +1 \end{bmatrix} \rightarrow S_{xgene} = \\ = \begin{bmatrix} -1 & -2 & -1 & 0 & 0 & 0 & +1 & +2 & +1 \end{bmatrix}. \tag{2}$$

2) EDGE DETECTOR FITNESS

For the fitness calculation, chromosomes are converted back to filter coefficients and applied to the training image forming a resulting edge image. The similarity of this image to the optimal edge image can be measured by finding the correlation between the two images [53], as defined by Equation 3.

$$Corr(x, y) = \frac{\sum_i \sum_j (x_{ij} - \mu_x)(y_{ij} - \mu_y)}{\sqrt{(\sum_i \sum_j (x_{ij} - \mu_x)^2)(\sum_i \sum_j (y_{ij} - \mu_y)^2)}}, \tag{3}$$

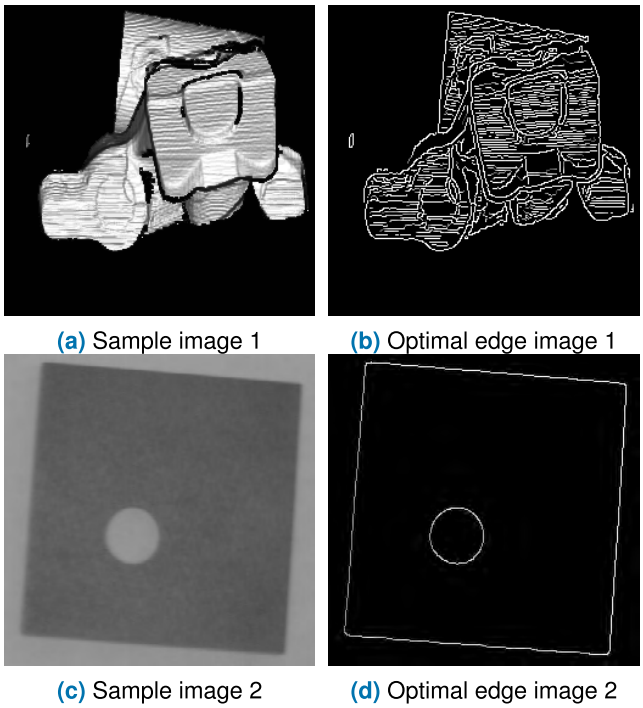

(a) Sample image 1 (b) Optimal edge image 1
(c) Sample image 2 (d) Optimal edge image 2

FIGURE 2. Sample training images.

TABLE 1. Confusion matrix defining the terms TP, TN, FP, and FN.

	Ground Truth	
Filter Output	Edge Pixel	Non-Edge Pixel
Edge Pixel	TP	FP
Non-Edge Pixel	FN	TN

where x and y are two image windows of common size $N \times N$ and μ_x and μ_y are the average of x and y respectively.

The structural similarity index (SSIM) [54] is also a performance measure. The SSIM index, defined by Equation 4, is designed to improve on traditional methods such as Peak Signal-to-Noise Ratio (PSNR) and Mean Squared Error (MSE).

$$SSIM(x, y) = \frac{(2\mu_x\mu_y + c_1)(2\sigma_{xy} + c_2)}{(\mu_x^2 + \mu_y^2 + c_1)(\sigma_x^2 + \sigma_y^2 + c_2)}, \tag{4}$$

where σ_x^2 and σ_y^2 are the variance of x and y, respectively. σ_{xy} is the covariance of x and y, $c_1 = (k_1\ L)^2$ and $c_2 = (k_2\ L)^2$ are two variables that stabilize a weak denominator division. L is the dynamic pixel value range $(2^b - 1)$ where b is the number of bits per pixel, $k_1 = 0.01$ and $k_2 = 0.03$ by default.

By appropriate weighting and combining, the correlation coefficient and SSIM can be utilized to compute a fitness value for a given solution, as represented by Equation 5.

$$Fitness = \lambda_1 Corr(x, y) + \lambda_2 SSIM(x, y), \tag{5}$$

TABLE 2. Different evaluation parameters calculation.

Parameter	P_{CD}	P_{ND}	P_{FA}	Accuracy	Sensitivity	Specificity
Formula	$\frac{TP}{RE_{Cnt}}$	$\frac{FN}{RE_{Cnt}}$	$\frac{FP}{RE_{Cnt}}$	$\frac{TP+TN}{TP+TN+FP+FN}$	$\frac{TP}{TP+FN}$	$\frac{TN}{TN+FP}$

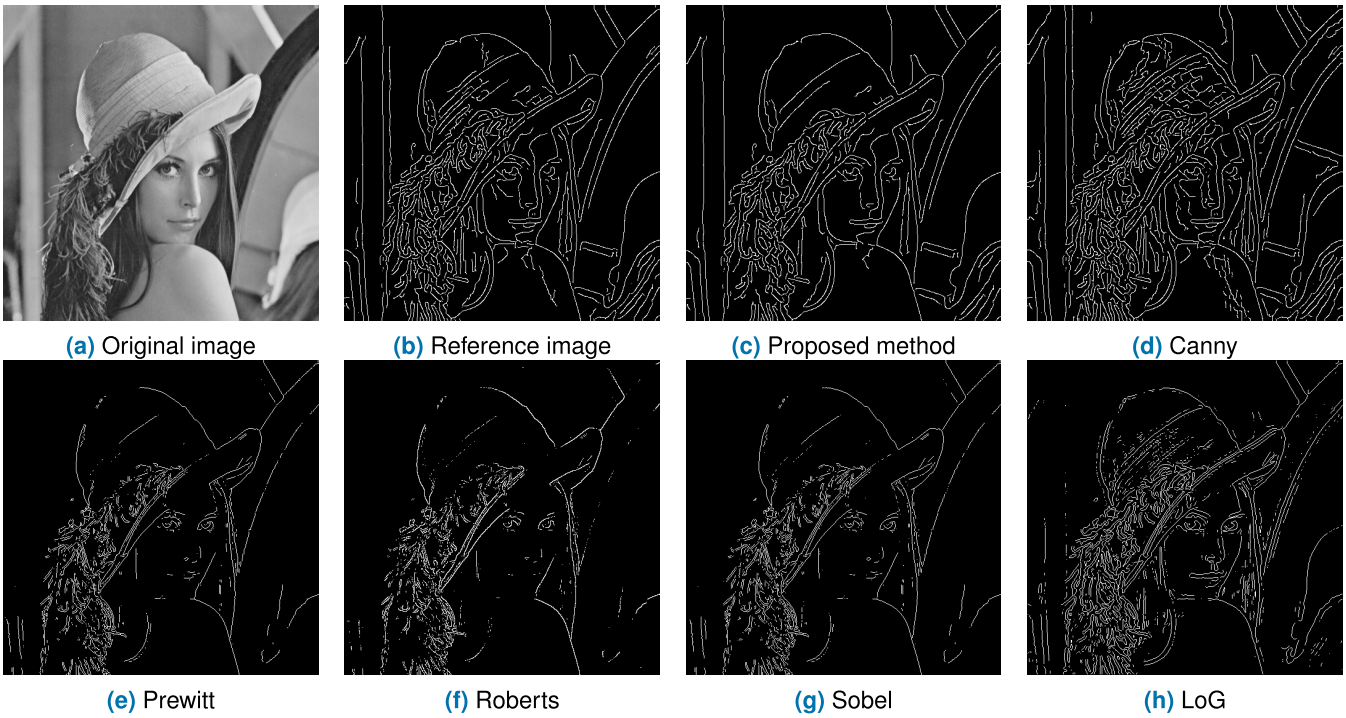

(a) Original image (b) Reference image (c) Proposed method (d) Canny

(e) Prewitt (f) Roberts (g) Sobel (h) LoG

FIGURE 3. Visual comparison among various edge detection methods.

TABLE 3. Performance analysis of Lena edge maps generated by classical edge detectors.

Method	Parameter										
	P_{CD}	P_{ND}	P_{FA}	Accuracy	Sensitivity	Specificity	FOM	Correlation	SSIM	MSE	PSNR
Proposed	0.8559	0.1441	0.0000	0.9909	0.8559	1.0000	0.8559	0.9207	0.9297	587.13	20.443
Canny	1.0000	0.0000	0.2260	0.9858	0.8210	0.9848	0.8396	0.8962	0.8882	921.01	18.488
Prewitt	0.2154	0.7845	0.2861	0.9329	0.2154	0.9808	0.4416	0.2727	0.6096	4362.4	11.733
Roberts	0.1731	0.8268	0.3012	0.9293	0.1731	0.9798	0.4134	0.2183	0.5835	4596.8	11.506
Sobel	0.2129	0.7870	0.2925	0.9323	0.2129	0.9804	0.4432	0.2676	0.6080	4398.9	11.697
LoG	0.3222	0.6777	0.5355	0.9239	0.3222	0.9642	0.6940	0.3077	0.5933	4944.1	11.189

where λ_1 and λ_2 are the weights of Correlation and SSIM,respectively.

One of the considerable performance measures of an edge detector is its immunity to noise. To factor this into the fitness function, the input images will also have different types of noise introduced to them. Edges will be detected and again will be compared to the reference edge image.

3) OPTIMAL EDGE IMAGE

To construct an optimal edge image, images of only edges will be created and filled-in appropriately to produce the input training images. The only-edge image can then be compared to outputs of edge detection attempts to determine how good they are. To enhance the performance, a set of 25 training images with different textures and density distribution is used

TABLE 4. Performance analysis of Lena edge maps generated by fractional edge detectors.

Method	Parameter										
	P_{CD}	P_{ND}	P_{FA}	Accuracy	Sensitivity	Specificity	FOM	Correlation	SSIM	MSE	PSNR
Proposed	0.8559	0.1441	0.0000	0.9909	0.8559	1.0000	0.8559	0.9207	0.9297	587.13	20.443
Mask 1 [22]	0.7241	0.2758	0.1220	0.9343	0.7241	0.9758	0.8231	0.7496	0.4717	4271.1	11.825
Mask 2 [23]	0.6673	0.3326	0.1093	0.9270	0.6673	0.9783	0.7260	0.7170	0.4059	4743.9	11.369
Mask 3 [24]	0.6990	0.3009	0.0741	0.9380	0.6990	0.9853	0.7601	0.7614	0.4594	4026.2	12.081
Mask 4 [25]	0.7099	0.2900	0.0833	0.9383	0.7099	0.9835	0.7779	0.7631	0.4698	4007.9	12.101
Mask 5 [26]	0.6955	0.3044	0.2932	0.9013	0.6955	0.9420	0.9026	0.6404	0.3514	6415.8	10.058

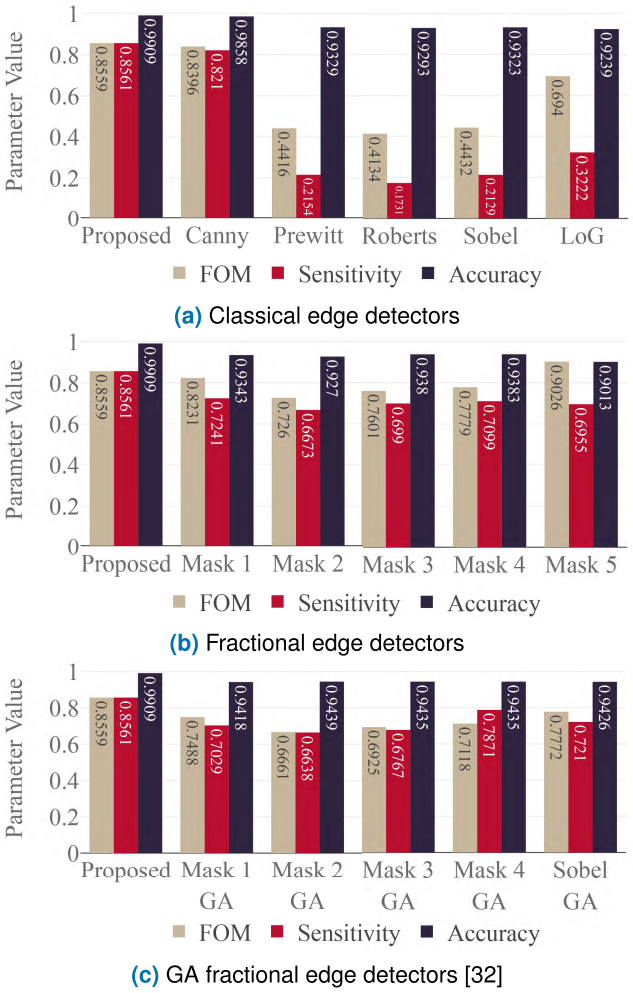

FIGURE 4. Comparison of edge map generation methods by key parameter.

during the training phase. Figure 2 presents a sample training image with its corresponding optimal edge image.

III. PERFORMANCE MEASURES

The performance of the proposed edge detection method can be evaluated in terms of accuracy, sensitivity, and specificity. The confusion matrix defining the terms TP, TN, FP, and FN from the proposed edge detection output and ground truth result for the calculation of accuracy, sensitivity, and specificity are shown in Table 1.

TP is the number of true positives, used to indicate the total number of edge pixels correctly classified. TN is the number of true negatives used to indicate non-edge pixels correctly classified. FP is the number of false-positive, used to indicate the wrongly detected or classified edge pixels when they are actually non-edge pixels. FN is the number of false negatives used to indicate the wrongly classified or detected non-edge pixels when they are actually edge pixels.

To evaluate the reliability and correctness of the edge map obtained by the proposed method, the following parameters are used to compare with the reference edge map: Percentage of detected pixels (P_{CD}), Percentage of not detected pixels (P_{ND}), Percentage of false alarms (P_{FA}). Sensitivity or true positive rate computes how many percentages of object pixels were correctly detected as object pixels. The range of metrics lies between 0 to 1, and the maximum value is optimal. Accuracy is the proportion of true results. It gives a percentage of how many objects and background pixels were exactly detected. If the accuracy value equals 1, then the output is the same as the input. Specificity or true negative rate measures the proportion of actual negatives that are correctly identified as such. Table 2 shows the formulas to calculate the mentioned parameters, where RE_{Cnt} represents the number of edge pixels in the reference map.

To quantitatively evaluate the performance of an edge detector, a criterion, that may help in judging the relative performance under controlled conditions, should be formulated. It's observed that in the response of an edge detector, there can be three types of errors: missing valid edges, errors in localizing edges, and classification of noise as edges. A Figure of Merit (FOM) for an edge detector should consider these three errors. One such FOM, called Pratt's figure of merit [55], is defined by Equation 6.

$$FOM = \frac{1}{max(I_A, I_I)} \sum_{i=1}^{RE_{Cnt}} \frac{1}{1 + \alpha \cdot d_i^2}, \tag{6}$$

TABLE 5. Performance analysis of Lena edge maps generated by GA optimized edge detectors.

Method	Parameter										
	P_{CD}	P_{ND}	P_{FA}	Accuracy	Sensitivity	Specificity	FOM	Correlation	SSIM	MSE	PSNR
Proposed	0.8559	0.1441	0.0000	0.9909	0.8559	1.0000	0.8559	0.9207	0.9297	587.13	20.443
Mask 1 GA [32]	0.7029	0.2971	0.0556	0.9418	0.7029	0.9890	0.7488	0.7761	0.4700	3786.1	12.349
Mask 2 GA [32]	0.6638	0.3362	0.0033	0.9439	0.6638	0.9993	0.6661	0.7864	0.4261	3644.8	12.514
Mask 3 GA [32]	0.6767	0.3233	0.0191	0.9435	0.6767	0.9962	0.6925	0.7835	0.4434	3675.3	12.478
Mask 4 GA [32]	0.6871	0.3129	0.0296	0.9435	0.6871	0.9941	0.7118	0.7831	0.4558	3676.5	12.476
Sobel GA [32]	0.7210	0.2790	0.0685	0.9426	0.7210	0.9865	0.7772	0.7801	0.4895	3730.1	12.414

TABLE 6. Performance analysis of Lena edge maps generated by classical edge detectors.

Method	Parameter				
	Mean	STD	Variance	Entropy	No. of corners
Reference	15.979	61.801	0.0145	0.3379	746
Proposed	13.676	57.450	0.0125	0.3016	651
Canny	19.591	67.911	0.0175	0.3909	928
Prewitt	8.0154	44.493	0.0075	0.2015	435
Roberts	7.5806	43.308	0.0071	0.1930	401
Sobel	8.0767	44.6579	0.0076	0.2027	448
LoG	13.706	57.510	0.0126	0.3021	708

TABLE 7. Performance analysis of Lena edge maps generated by fractional edge detectors.

Method	Parameter				
	Mean	STD	Variance	Entropy	No. of corners
Reference	15.979	61.801	0.0145	0.3379	746
Proposed	13.676	57.450	0.0125	0.3016	651
Mask 1 [22]	35.620	88.399	0.1464	0.5834	112
Mask 2 [23]	32.696	85.255	0.1362	0.5525	43
Mask 3 [24]	32.548	85.090	0.1356	0.5509	102
Mask 4 [25]	33.394	86.025	0.1386	0.5600	112
Mask 5 [26]	41.623	94.241	0.1664	0.6419	174

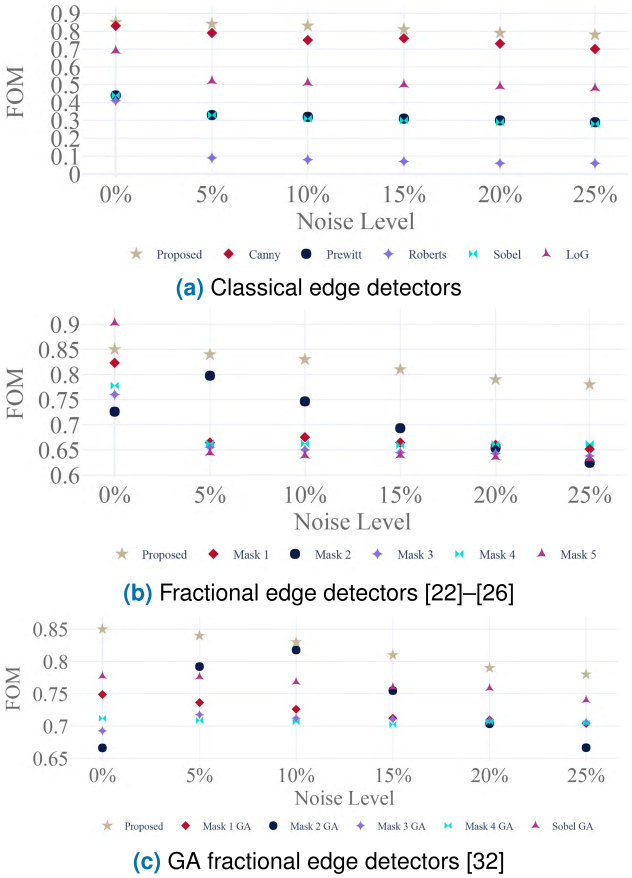

FIGURE 5. Estimation of the decrease in the values of Figure of Merit (FOM) in relation to the noise level for different methods.

where I_A, I_I, d_i, and α are the detected edges, ideal edges, the distance between the actual and ideal edges, and a design constant used to penalize displaced edges, respectively. (By default, $\alpha = \frac{1}{9}$, the optimal value established by Abdou and Pratt [55]).

Other metrics such as Mean squared error (MSE), Peak signal-to-noise ratio (PSNR), Correlation Coefficient, defined by Equation 3, and SSIM, defined by Equation 4, are also assessed for evaluating the performance of the proposed method.

The classical statistical measures, such as Mean, Standard Deviation, Variance (VAR), and Entropy, are also calculated. The value of mean is the measure of average gray levels. A measure of average contrast is given by standard deviation, while entropy, given by Equation 7, measures randomness and information contained in an image.

$$e = -\sum_{i=0}^{L-1} p_i(\log_2 p_i), \tag{7}$$

TABLE 8. Performance analysis of Lena edge maps generated by GA optimized edge detectors.

Method	Parameter				
	Mean	STD	VAR	Entropy	No. of corners
Mask 1 GA [32]	31.932	84.398	0.1335	0.5442	98
Mask 2 GA [32]	28.080	79.824	0.1194	0.5003	15
Mask 3 GA [32]	29.289	81.307	0.1239	0.5144	56
Mask 4 GA [32]	30.173	82.363	0.1271	0.5245	75
Sobel GA [32]	33.232	85.847	0.1381	0.5583	92

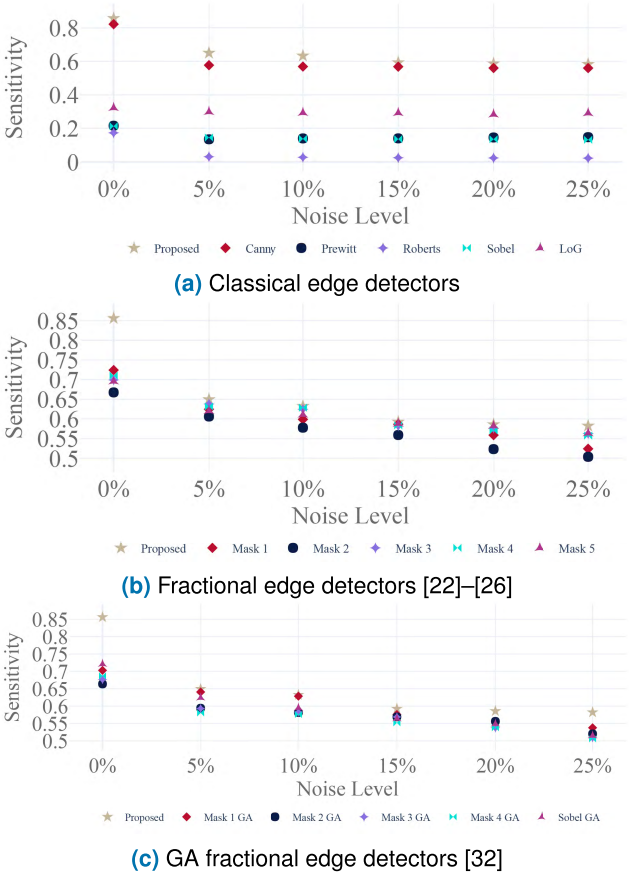

(a) Classical edge detectors

(b) Fractional edge detectors [22]–[26]

(c) GA fractional edge detectors [32]

FIGURE 6. Estimation of the decrease in the values of Sensitivity in relation to the noise level for different methods.

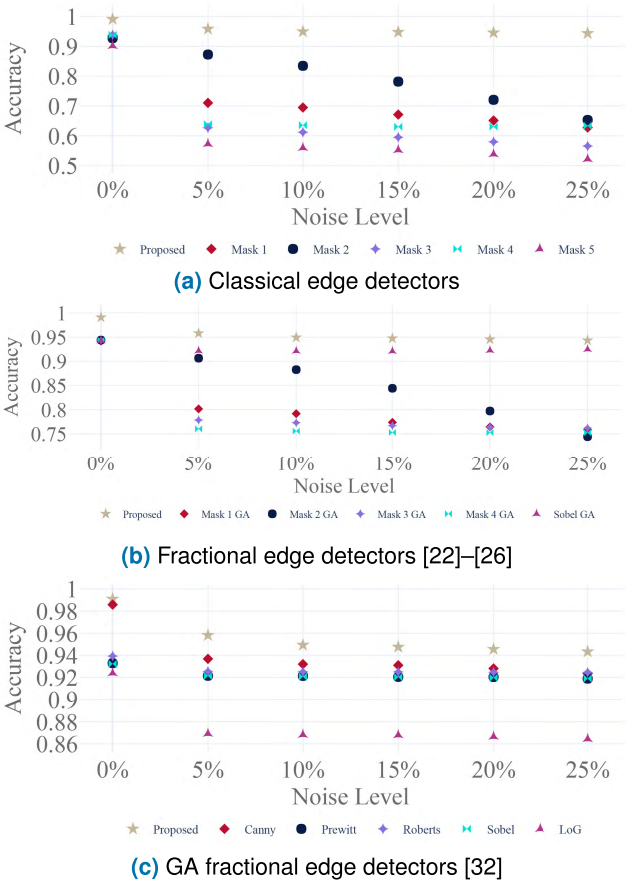

(a) Classical edge detectors

(b) Fractional edge detectors [22]–[26]

(c) GA fractional edge detectors [32]

FIGURE 7. Estimation of the decrease in the values of Accuracy in relation to the noise level for different methods.

where, p_i is the probability distribution of i number of gray levels where $i = 0, 1, 2, \ldots L$ and L denotes the maximum number of gray levels.

To test the robustness to noise, the test images are corrupted with different levels of additive Gaussian noise. Then, the proposed method is applied to the noisy images and the parameters are calculated for each noise level.

IV. RESULTS AND DISCUSSION

In this section, the results of the proposed edge detection method are compared both qualitatively (i.e. visually) and quantitatively with those obtained by various classical edge detection filters, Fractional-Order filters [22]–[26], and GA optimized Fractional-Order filters [32]. Initially, the simulations are performed on the standard image of Lena of pixel size 512 × 512 with a gray-scale map of 256 gray levels. All evaluation parameters during the study are calculated with the help of a reference image. Since there is no standard reference image, a reference image for Lena is created by averaging the edge maps obtained by the classical edge detectors.

A. QUALITATIVE ANALYSIS

The texture results as qualitative (i.e. visual) comparison among various edge detection methods are presented in Figure 3.

It is observed from the figure, in which regions generated by Prewitt, Roberts, Sobel, and LoG edge detectors have openings, while the Canny edge detector gives many false lines due to its over-sensitive nature. The results indicate that the edges generated by the proposed method are closer to the reference edge map than the conventional methods.

B. QUANTITATIVE ANALYSIS

The test performance of the proposed edge detection method is determined by the computation of statistical parameters such as P_{CD}, P_{ND}, P_{FA}, sensitivity, specificity, and accu-

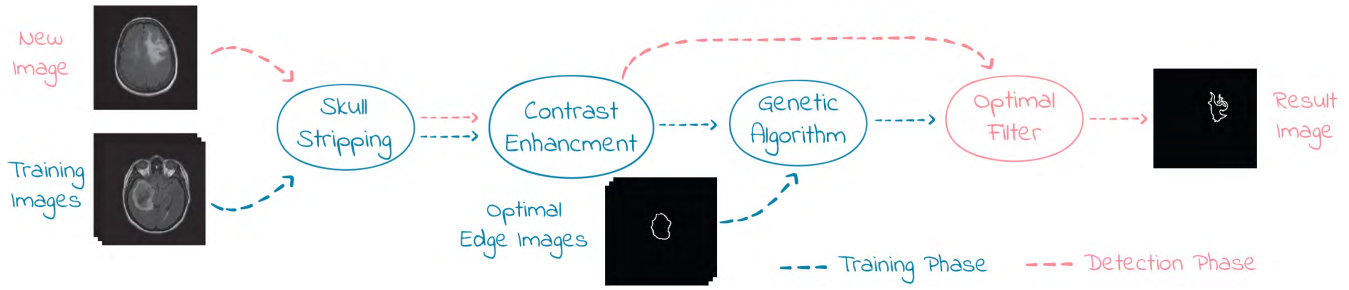

FIGURE 8. Proposed Brain Tumor Detection Method.

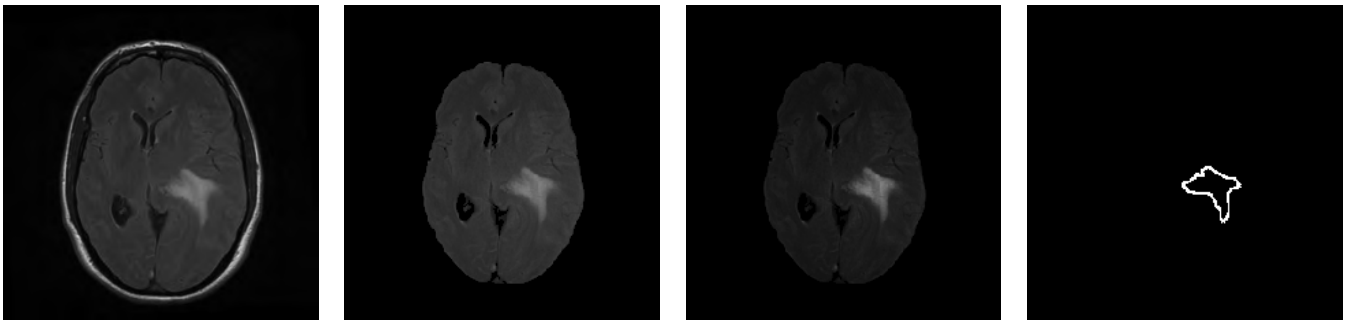

FIGURE 9. Brain tumor detection pipeline.

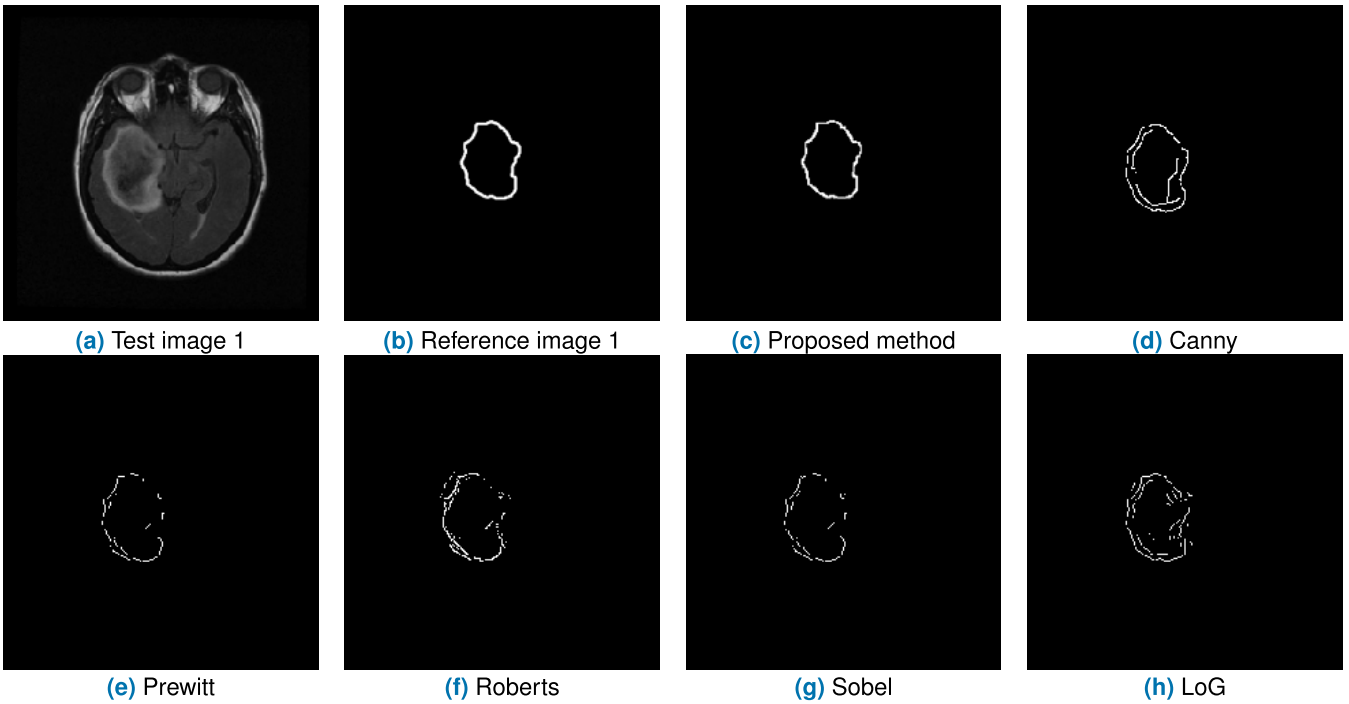

FIGURE 10. Visual comparison among various edge detectors when tested on test image 1.

racy, defined in Table 2, in comparison with the various edge detection methods as shown in tables 3 to 5. Higher values of accuracy, sensitivity, and specificity indicate better performance. From these tables, the performance of the proposed edge detection method is better than the classical methods.

The proposed method achieved an average accuracy of 99.09%, an average of Pratt's Figure of Merit (FOM) value

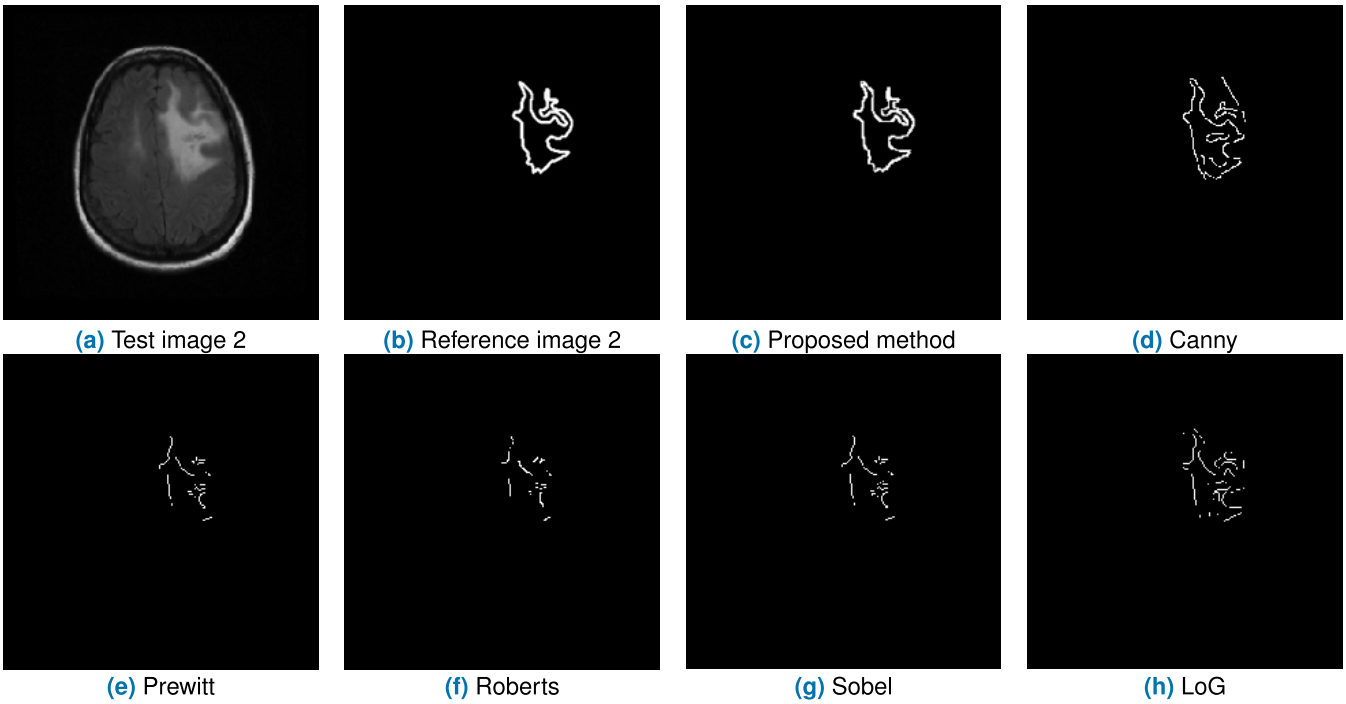

FIGURE 11. Visual comparison among various edge detectors when tested on test image 2.

TABLE 9. Performance analysis of test image 1 (shown in Figure 10a) edge maps generated by classical edge detectors.

Test image 1											
	Parameter										
Method	P_{CD}	P_{ND}	P_{FA}	Accuracy	Sensitivity	Specificity	FOM	Correlation	SSIM	MSE	PSNR
Proposed	0.9585	0.0415	0.0005	0.9949	0.9585	0.9999	0.9000	0.9876	0.9868	166.744	25.910
Canny	0.9243	0.0757	0.0219	0.9881	0.9243	0.9970	0.7875	0.9542	0.9567	613.34	20.254
Prewitt	0.9157	0.0843	0.0040	0.9893	0.9157	0.9994	0.7093	0.9642	0.9633	478.85	21.329
Roberts	0.9220	0.0780	0.0129	0.9889	0.9220	0.9982	0.7373	0.9598	0.9597	538.43	20.820
Sobel	0.9157	0.0843	0.0045	0.9892	0.9157	0.9994	0.7093	0.9640	0.9629	481.87	21.302
LoG	0.9205	0.0795	0.0162	0.9884	0.9205	0.9978	0.7875	0.9582	0.9538	559.70	20.651

of 85.59%, and an average sensitivity of 85.59%. Tables 3 to 5 also provide the details of the different performance parameters such as the Correlation coefficient, structured similarity index (SSIM), Mean Squared Error (MSE) and peak signal-to-noise ratio (PSNR). A higher value of Correlation and SSIM indicates proper detection. At the same time, a lower value of MSE and a higher value of PSNR indicate better signal-to-noise ratio in the extracted image.

The statistical parameters such as mean, variance, and standard deviation are also calculated and summarized in tables 6 to 8. They show that the number of corners of the edge map obtained from the proposed method is closer to that of reference edge map than all other methods.

Figure 4 represents the comparative plots of the average values of Pratt's Figure of Merit (FOM), sensitivity, and accuracy characteristics for the standard Lena image. The results indicate that the proposed edge detection method can bring its efficiency to 99.09% of accuracy, which is considered a very high rate and sensitivity of 85.61%, outperforming all the other methods. Pratt's Figure of Merit (FOM) should be high for effective edge detection images, so the proposed method gives an excellent value of 85.59% when compared to other edge detection methods.

Figures 5, 6 and 7 present results from the various methods when tested on the noisy Lena images. Results denote that the proposed edge detection method has better noise immunity in edge detection compared to other operators. It doesn't

TABLE 10. Performance analysis of test image 2 (shown in Figure 11a) edge maps generated by classical edge detectors.

Test image 2											
	Parameter										
Method	P_{CD}	P_{ND}	P_{FA}	Accuracy	Sensitivity	Specificity	FOM	Correlation	SSIM	MSE	PSNR
Proposed	0.9326	0.0674	0.0011	0.9910	0.9326	0.9998	0.8714	0.9784	0.9799	304.816	23.290
Canny	0.8637	0.1363	0.0199	0.9794	0.8637	0.9970	0.8232	0.9274	0.9407	1011.08	18.083
Prewitt	0.8448	0.1552	0.0036	0.9791	0.8448	0.9995	0.7234	0.9336	0.9451	926.35	18.463
Roberts	0.8422	0.1578	0.0028	0.9788	0.8422	0.9996	0.7379	0.9314	0.9441	955.87	18.327
Sobel	0.8445	0.1555	0.0040	0.9790	0.8445	0.9994	0.7234	0.9332	0.9450	930.99	18.441
LoG	0.8532	0.1468	0.0067	0.9798	0.8532	0.9990	0.7994	0.9334	0.9429	927.47	18.458

TABLE 11. Performance analysis of test image 1 (shown in Figure 10a) edge maps generated by fractional edge detectors.

Test image 1											
	Parameter										
Method	P_{CD}	P_{ND}	P_{FA}	Accuracy	Sensitivity	Specificity	FOM	Correlation	SSIM	MSE	PSNR
Proposed	0.9326	0.0674	0.0011	0.9910	0.9326	0.9998	0.8714	0.9784	0.9799	304.816	23.290
Mask 1 [22]	0.8110	0.0794	0.0056	0.9380	0.8110	0.9758	0.8655	0.8041	0.5007	1213.0	14.988
Mask 2 [23]	0.7474	0.0957	0.0051	0.9307	0.7474	0.9783	0.7634	0.7692	0.4309	1347.3	14.41
Mask 3 [24]	0.7829	0.0866	0.0034	0.9418	0.7829	0.9853	0.7993	0.8168	0.4876	1143.4	15.313
Mask 4 [25]	0.7951	0.0835	0.0039	0.9421	0.7951	0.9835	0.8180	0.8186	0.3287	1138.2	15.338
Mask 5 [26]	0.7789	0.0876	0.0136	0.9049	0.7789	0.9420	0.9491	0.6870	0.3730	1822.1	12.748

TABLE 12. Performance analysis of test image 2 (shown in Figure 11a) edge maps generated by fractional edge detectors.

Test image 2											
	Parameter										
Method	P_{CD}	P_{ND}	P_{FA}	Accuracy	Sensitivity	Specificity	FOM	Correlation	SSIM	MSE	PSNR
Proposed	0.9326	0.0674	0.0011	0.9910	0.9326	0.9998	0.8714	0.9784	0.9799	304.816	23.290
Mask 1 [22]	0.7890	0.1291	0.0139	0.9343	0.789	0.9757	0.838	0.7967	0.3272	2217.4	13.472
Mask 2 [23]	0.7272	0.1557	0.0124	0.927	0.7272	0.9782	0.7391	0.762	0.4279	2462.9	12.953
Mask 3 [24]	0.7617	0.1408	0.0084	0.9381	0.7617	0.9852	0.7739	0.8092	0.4842	2090.2	13.764
Mask 4 [25]	0.7735	0.1357	0.0095	0.9384	0.7735	0.9834	0.792	0.8110	0.3253	2080.7	13.787
Mask 5 [26]	0.7578	0.1425	0.0334	0.9013	0.7578	0.9419	0.9189	0.6806	0.3704	3330.8	11.459

only perform reasonably well in noisy environments but also provides good edges.

From these figures, the FOM and accuracy values almost do not change with the increasing noise level. The change is less than one percent for a noise level lower than 25%. However, the sensitivity index shows a more marked decrease.

V. PROPOSED BRAIN TUMOR DETECTION METHOD

In most cases, images (or image sets) obtained from medical devices have noticeable noise caused by technological features of device operation. This paper suggests the following procedure to process the medical images. Two main steps are performed on the input grayscale MRI scan image, Image Enhancement, and Edge Detection. After completing

TABLE 13. Performance analysis of test image 1 (shown in Figure 10a) edge maps generated by GA optimized edge detectors.

Test image 1											
	Parameter										
Method	P_{CD}	P_{ND}	P_{FA}	Accuracy	Sensitivity	Specificity	FOM	Correlation	SSIM	MSE	PSNR
Proposed	0.9326	0.0674	0.0011	0.9910	0.9326	0.9998	0.8714	0.9784	0.9799	304.816	23.290
Mask 1 GA [32]	0.7872	0.0855	0.0026	0.9455	0.7872	0.9889	0.7874	0.8325	0.3289	1075.2	15.651
Mask 2 GA [32]	0.7434	0.0967	0.0002	0.9476	0.7434	0.9992	0.7004	0.8435	0.4523	1035.1	15.86
Mask 3 GA [32]	0.7578	0.0930	0.0009	0.9472	0.7578	0.9961	0.7282	0.8404	0.4706	1043.8	15.815
Mask 4 GA [32]	0.7695	0.09	0.0014	0.9472	0.7695	0.994	0.7485	0.8400	0.4838	1044.1	15.812
Sobel GA [32]	0.8075	0.0803	0.0032	0.9463	0.8075	0.9864	0.8172	0.8368	0.5196	1059.3	15.734

TABLE 14. Performance analysis of test image 2 (shown in Figure 11a) edge maps generated by GA optimized edge detectors.

Test image 2											
	Parameter										
Method	P_{CD}	P_{ND}	P_{FA}	Accuracy	Sensitivity	Specificity	FOM	Correlation	SSIM	MSE	PSNR
Proposed	0.9326	0.0674	0.0011	0.9910	0.9326	0.9998	0.8714	0.9784	0.9799	304.816	23.290
Mask 1 GA [32]	0.7659	0.1390	0.0063	0.9418	0.7659	0.9888	0.7624	0.8247	0.3254	1965.6	14.069
Mask 2 GA [32]	0.7233	0.1573	0.0004	0.9439	0.7233	0.9991	0.6782	0.8357	0.4491	1892.2	14.257
Mask 3 GA [32]	0.7373	0.1513	0.0022	0.9435	0.7373	0.9960	0.705	0.8326	0.4673	1908.1	14.216
Mask 4 GA [32]	0.7486	0.1464	0.0034	0.9435	0.7486	0.9939	0.7247	0.8322	0.4804	1908.7	14.213
Sobel GA [32]	0.7856	0.1306	0.0078	0.9426	0.7856	0.9863	0.7913	0.8290	0.5159	1936.5	14.143

TABLE 15. Performance analysis of test image 1 and 2 (shown in Figure 10a and Figure 11a)edge maps generated by classical edge detectors.

	Test image 1					Test image 2				
	Parameter					Parameter				
Method	Mean	STD	Variance	Entropy	No. of corners	Mean	STD	Variance	Entropy	No. of corners
Proposed	29.734	81.841	0.1255	0.5195	15	31.363	83.749	0.1314	0.5379	22
Canny	29.337	81.365	0.1241	0.515	18	29.681	81.778	0.1253	0.5189	22
Prewitt	28.515	80.363	0.121	0.5054	17	28.496	80.339	0.121	0.5052	15
Roberts	28.988	80.942	0.1228	0.5109	18	28.386	80.204	0.1205	0.5039	15
Sobel	28.529	80.381	0.1211	0.5056	17	28.501	80.345	0.121	0.5052	15
LoG	29.041	81.006	0.123	0.5115	20	28.883	80.814	0.1224	0.5097	19

the image enhancement, the final step is a formation of the edge map using the proposed edge detection method. Figure 8 shows a block diagram for the proposed brain tumour detection method.

A. IMAGE ENHANCEMENT

During the image enhancement step, the skull stripping and contrast enhancement are conducted. To improve the contrast by highlighting the area of interest, Balance Contrast Enhancement Technique (BCET) technique is used.

B. SKULL STRIPPING

The skull stripping method is the process of removal of non-brain tissues, like skull, scalp, dura, eyes, etc. from brain MR images. It is used as an essential preprocessing step in many brain MR image processing applications.

TABLE 16. Performance analysis of test image 1 and 2 (shown in Figure 10a and Figure 11a)edge maps generated by fractional edge detectors.

	Test image 1					Test image 2				
	Parameter					Parameter				
Method	Mean	STD	Variance	Entropy	No. of corners	Mean	STD	Variance	Entropy	No. of corners
Proposed	29.734	81.841	0.1255	0.5195	15	31.363	83.749	0.1314	0.5379	22
Mask 1 [22]	16.385	62.054	0.0147	0.3387	11	15.534	60.64	0.014	0.3272	19
Mask 2 [23]	15.04	59.847	0.0137	0.3208	9	14.258	58.484	0.013	0.3098	15
Mask 3 [24]	14.972	59.731	0.0136	0.3199	10	14.194	58.37	0.013	0.3089	18
Mask 4 [25]	15.361	60.387	0.0139	0.3252	12	14.563	59.011	0.0133	0.3141	17
Mask 5 [26]	19.146	66.155	0.0167	0.3727	13	18.151	64.648	0.0159	0.36	14

TABLE 17. Performance analysis of test image 1 and 2 (shown in Figure 10a and Figure 11a)edge maps generated by GA optimized edge detectors.

	Test image 1					Test image 2				
	Parameter					Parameter				
Method	Mean	STD	Variance	Entropy	No. of corners	Mean	STD	Variance	Entropy	No. of corners
Proposed	29.734	81.841	0.1255	0.5195	15	31.363	83.749	0.1314	0.5379	22
Mask 1 GA [32]	14.688	59.245	0.0134	0.316	12	13.925	57.895	0.0128	0.3052	17
Mask 2 GA [32]	12.916	56.034	0.012	0.2905	8	12.245	54.758	0.0114	0.2806	15
Mask 3 GA [32]	13.472	57.075	0.0124	0.2987	10	12.772	55.775	0.0119	0.2885	16
Mask 4 GA [32]	13.879	57.817	0.0127	0.3045	9	13.158	56.499	0.0122	0.2941	17
Sobel GA [32]	15.286	60.262	0.0139	0.3242	13	14.492	58.889	0.0132	0.3131	19

For example, during the Edge Detection of brain tumours, the skull stripping algorithm is incorporated to identify the region of interest [56].

C. CONTRAST ENHANCEMENT

In the proposed methodology, BCET technique is used [57]. The contrast of the image can be stretched or compressed without changing the histogram pattern of the input image. The solution is based on the parabolic function obtained from the input image. The general form of the parabolic function is defined by Equation 8a.

$$I_{enhanced} = a(I - b)^2 + c, \tag{8a}$$

Coefficients a, b and c are calculated using the minimum and maximum intensity values of the input image I, the minimum and maximum intensity values of the output image ($I_{enhanced}$), and mean value of intensity of the output image (E):

$$a = \frac{H - L}{(h - l)(h + l - 2b)}, \tag{8b}$$

$$b = \frac{h^2(E - L) - s(H - L) + l^2(H - E)}{2[h(E - L) - e(H - L) + l(H - E)]}, \tag{8c}$$

$$c = L - a(l - b)^2, \tag{8d}$$

where l and h are the minimum and the maximum intensity values of the input image respectively, e is the mean value of intensity the input image. L and H are the minimum and the maximum intensity values of the output image. s denotes the mean square sum of intensity of the input image and given by Equation 8e.

$$s = \frac{1}{N}\sum_{i=1}^{N} I^2(i). \tag{8e}$$

D. EDGE DETECTION

The edges in an image can be generated using complex algorithms, such as LoG and Canny; even with the easier ones, for example, Prewitt, Roberts, and Sobel. However, the accuracy of the work depends on the original image. The image after enhancement has many levels of intensity gradation that, during an edge detection, can lead to the formation of false edge fragments and so on. Taking this into account, the proposed GA Edge Detection method is trained with the appropriate training MR images. The obtained Edge Detector is then applied to the region of interest (ROI) i.e. the region in the MR image which contains the tumour.

The training dataset contains brain MR images together with manual FLAIR abnormality segmentation masks. The images were obtained from The Cancer Imaging Archive

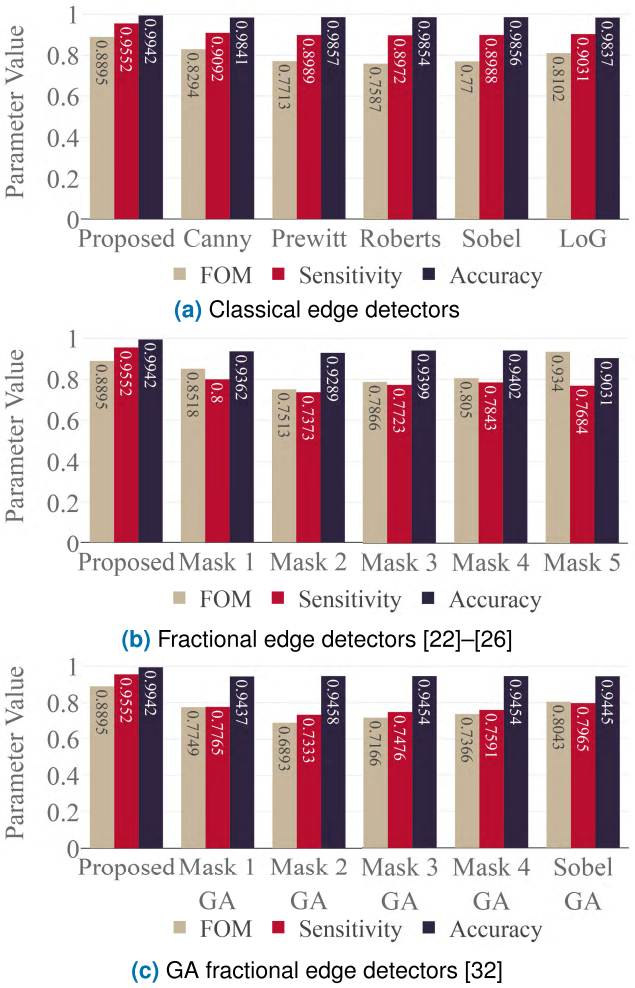

FIGURE 12. Comparison of edge map generation methods by key parameter.

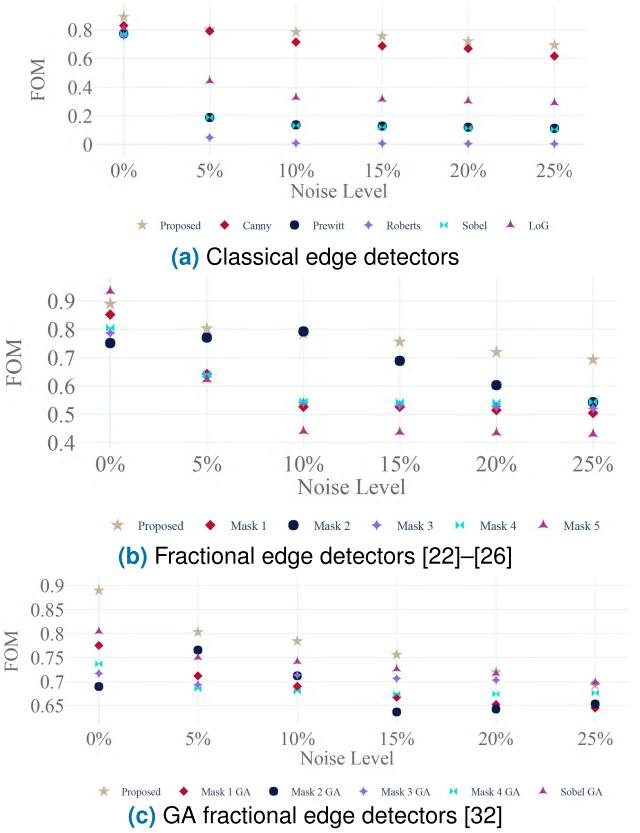

FIGURE 13. Estimation of the decrease in the values of Figure of Merit (FOM) in relation to the noise level for different methods.

(TCIA) [58]. They correspond to 110 patients included in The Cancer Genome Atlas (TCGA) lower-grade glioma collection. With a simple contour detection operation, the optimal edge image is obtained.

The sample experimental results obtained from the proposed methodology are depicted in Figure 9. It shows the original image along with the skull-stripped image, enhanced image after contrast enhancement, and the final edge map obtained by applying the proposed edge detection method on the Region of Interest (ROI) i.e. the region in the MR scan image which contains the tumour.

E. EVALUATION OF PROPOSED TUMOR DETECTION METHOD

To evaluate the brain tumour detection method, 50 images were selected. Medical images contain tumours characterized by different locations and different types of pathologies, shape, size, density, as well as the size of the area of the affected tissue near the tumour space.

To show the capabilities of the proposed methodology, various studies are carried out. The first study implies comparing the proposed method with classical approaches for edge detection based on simple gradient operators such as Roberts, Prewitt, Sobel, and complex methods such as LoG and Canny. The proposed method is also compared with fractional-order masks [22]–[26] and GA optimized fractional-order filters introduced in the literature [32].

From the results, the regions of Prewitt, Roberts, Sobel, and LoG edge detection don't give closed contour; resulting in false tumours. On the other hand, Canny edge detection gives additional unnecessary lines because of its over-sensitive nature. The proposed method generates well-closed contours with fine boundaries. Thus, the extracted tumour from the proposed method is very close to the original tumour.

One limitation of the proposed method is that the accuracy of the detections depends mainly on the selected training images. Moreover, as the proposed method learns from the training examples, the training time is a function of the number of training images used. However, the number of training images can be varied to obtain an accuracy-speed tradeoff.

1) QUALITATIVE ANALYSIS

For the purpose of subjective quality evaluation, figs. 10 and 11 shows the texture results as qualitative comparison among various methods.

2) QUANTITATIVE ANALYSIS

For the two test images shown in figs. 10a and 11a, the result obtained using the proposed brain tumour detection method

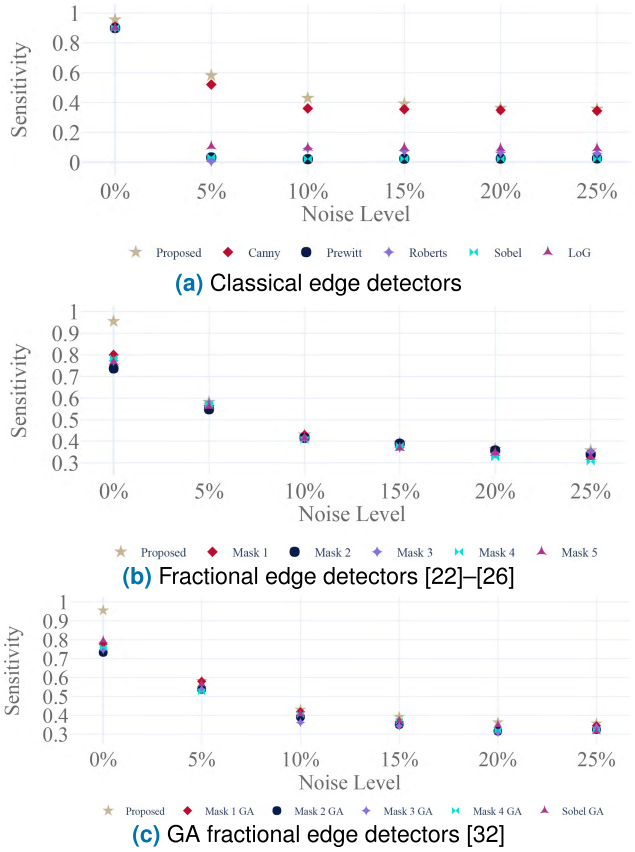

FIGURE 14. Estimation of the decrease in the values of Sensitivity in relation to the noise level for different methods.

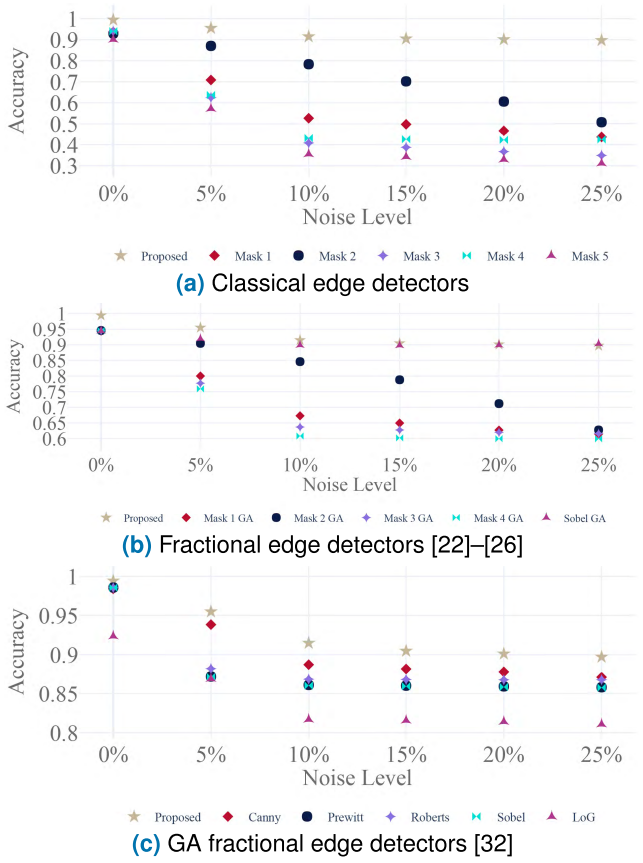

FIGURE 15. Estimation of the decrease in the values of Accuracy in relation to the noise level for different methods.

based on Genetic Algorithm optimization is compared with the number of edge detectors. This is based on performance measures such as sensitivity, specificity, accuracy, and Pratt's Figure of Merit (FOM). The detailed analysis of performance measures is shown in tables 9 to 14 along with Correlation coefficient, Structural Similarity Index (SSIM), MSE, and PSNR. Tables 15 and 17 show the statistical measures such as Mean, standard deviation, Variance (VAR), Entropy, and the number of corners.

The proposed tumour detection method achieved an average accuracy of 99.61%, an average of Pratt's Figure of Merit (FOM) value of 89.88%, and an average sensitivity of 98.71%, demonstrating the effectiveness of the proposed method for detecting brain tumour edges from MRI scans.

Figure 12 represents the detailed comparative plots of the average values of the FOM, sensitivity, accuracy, and specificity characteristics for a test dataset of 50 images, and the performance of the proposed tumour detection method is better than other classical methods and filters from literature.

Through the performance measure, it is depicted that the performance of the proposed methodology has significantly improved the tumour identification compared with other methods. Even a modest improvement in the sensitivity parameter is very important and critical for a radiologist or clinical doctor for surgical planning. Figures 13 to 15 present the average results from the various methods when tested on 50 noisy test images.

The figures show that the FOM values almost do not change with the increasing noise level. However, this time and unlike what happened with Lena's image, accuracy and sensitivity indexes show a more marked decrease.

VI. CONCLUSION

In this paper, a Genetic Algorithm (GA) was effectively used to determine an optimal edge detection method. The algorithm takes various training images and their corresponding optimal edge images, then it outputs an optimal edge filter and thresholding algorithm. The visual and quantitative comparison of edge detection algorithms was performed. The proposed method provided good localization and detected sharper edges as compared to other conventional and fractional-order methods. The proposed method brought its efficiency with an accuracy of 99.09%, FOM of 85.59%. The paper also proposed a Tumor detection method based on the proposed Edge detection method preceded by some image enhancement operations. A qualitative and quantitative analysis was then performed between the classical, fractional, threshold-optimized edge detection method, and the proposed brain tumour detection method. From the experimental results performed on the different images, it is clear

that the analysis for brain tumour detection is fast and accurate when compared with the manual detection performed by radiologists or clinical experts. The experimental results achieved 99.61% accuracy demonstrating the effectiveness of the proposed method for detecting brain tumours from MR images.

REFERENCES

[1] L. G. Roberts, "Machine perception of three-dimensional solids," Ph.D. dissertation, Massachusetts Inst. Technol., Cambridge, MA, USA, 1963.
[2] J. M. Prewitt, "Object enhancement and extraction," *Picture Process. Psychopictorics*, vol. 10, no. 1, pp. 15–19, 1970.
[3] K. Engel, M. Hadwiger, J. M. Kniss, and C. Rezk-Salama, "Real-time volume graphics," in *Eurographics*, N. Magnenat-Thalmann and K. Buhler, Eds. The Eurographics Association, 2006.
[4] I. Sobel and G. Feldman, "A 3 × 3 isotropic gradient operator for image processing," *Talk Stanford Artif. Project*, pp. 271–272, 1968.
[5] J. S. Chen, A. Huertas, and G. Medioni, "Fast convolution with Laplacian-of-Gaussian masks," *IEEE Trans. Pattern Anal. Mach. Intell.*, vol. PAMI-9, no. 4, pp. 584–590, Jul. 1987.
[6] D. Demigny, "On optimal linear filtering for edge detection," *IEEE Trans. Image Process.*, vol. 11, no. 7, pp. 728–737, Jul. 2002.
[7] L. Ding and A. Goshtasby, "On the Canny edge detector," *Pattern Recognit.*, vol. 34, no. 3, pp. 721–725, Mar. 2001.
[8] R. Medina-Carnicer, A. Carmona-Poyato, R. Muñoz-Salinas, and F. J. Madrid-Cuevas, "Determining hysteresis thresholds for edge detection by combining the advantages and disadvantages of thresholding methods," *IEEE Trans. Image Process.*, vol. 19, no. 1, pp. 165–173, Jan. 2020.
[9] K. B. Oldman and J. Spanier, *The Fractional Calculus: Theory and Applications of Differentiation and Integration to Arbitrary Order*. Mineola, NY, USA: Dover, 2006.
[10] A. Kilbas, H. Srivastava, and J. Trujillo, *Theory and Applications Of Fractinal Differential Equations*, vol. 204. Alpharetta, GA, USA: Elsevier Science Inc., Jan. 2006.
[11] A. AboBakr, L. A. Said, A. H. Madian, A. S. Elwakil, and A. G. Radwan, "Experimental comparison of integer/fractional-order electrical models of plant," *AEU-Int. J. Electron. Commun.*, vol. 80, pp. 1–9, Oct. 2017.
[12] A. Allagui, T. J. Freeborn, A. S. Elwakil, M. E. Fouda, B. J. Maundy, A. G. Radwan, Z. Said, and M. A. Abdelkareem, "Review of fractional-order electrical characterization of supercapacitors," *J. Power Sources*, vol. 400, pp. 457–467, Oct. 2018.
[13] S. M. Ismail, L. A. Said, A. G. Radwan, A. H. Madian, and M. F. Abu-ElYazeed, "A novel image encryption system merging fractional-order edge detection and generalized chaotic maps," *Signal Process.*, vol. 167, Feb. 2020, Art. no. 107280.
[14] M. F. Tolba, L. A. Said, A. H. Madian, and A. G. Radwan, "FPGA implementation of the fractional order integrator/differentiator: Two approaches and applications," *IEEE Trans. Circuits Syst. I, Reg. Papers*, vol. 66, no. 4, pp. 1484–1495, Apr. 2019.
[15] D. A. Yousri, A. M. Abdelaty, L. A. Said, A. S. Elwakil, B. Maundy, and A. G. Radwan, "Parameter identification of fractional-order chaotic systems using different meta-heuristic optimization algorithms," *Nonlinear Dyn.*, vol. 95, no. 3, pp. 2491–2542, Feb. 2019.
[16] A. M. Abdelaty, M. Roshdy, L. A. Said, and A. G. Radwan, "Numerical simulations and FPGA implementations of fractional-order systems based on product integration rules," *IEEE Access*, vol. 8, pp. 102093–102105, 2020, doi: 10.1109/ACCESS.2020.2997765.
[17] B. M. Aboalnaga, L. A. Said, A. H. Madian, A. S. Elwakil, and A. G. Radwan, "Cole bio-impedance model variations in *Daucus Carota Sativus* under heating and freezing conditions," *IEEE Access*, vol. 7, pp. 113254–113263, 2019, doi: 10.1109/ACCESS.2019.2934322.
[18] S. M. Ismail, L. A. Said, A. A. Rezk, A. G. Radwan, A. H. Madian, M. F. Abu-Elyazeed, and A. M. Soliman, "Generalized fractional logistic map encryption system based on FPGA," *AEU-Int. J. Electron. Commun.*, vol. 80, pp. 114–126, Oct. 2017.
[19] Q. Yang, D. Chen, T. Zhao, and Y. Chen, "Fractional calculus in image processing: A review," *Fractional Calculus Appl. Anal.*, vol. 19, no. 5, pp. 1222–1249, Jan. 2016.
[20] O. Li and P.-L. Shui, "Noise-robust color edge detection using anisotropic morphological directional derivative matrix," *Signal Process.*, vol. 165, pp. 90–103, Dec. 2019.
[21] A. Sengupta, A. Seal, C. Panigrahy, O. Krejcar, and A. Yazidi, "Edge information based image fusion metrics using fractional order differentiation and sigmoidal functions," *IEEE Access*, vol. 8, pp. 88385–88398, 2020.
[22] D. Tian, J. Wu, and Y. Yang, "A fractional-order Sobel operator for medical image structure feature extraction," *Adv. Mater. Res.*, vols. 860–863, pp. 5173–5176, May 2014.
[23] Z. Yang, F. Lang, X. Yu, and Y. Zhang, "The construction of fractional differential gradient operator," *J. Comput. Inf. Syst.*, vol. 7, no. 12, pp. 4328–4342, Dec. 2011.
[24] Y. Pu, "Fractional calculus approach to texture of digital image," in *Proc. 8th Int. Conf. Signal Process.*, Nov. 2006, pp. 1–6.
[25] J.-L. Chen, C.-H. Lin, Y.-C. Du, and C.-H. Huang, "Combining fractional-order edge detection and chaos synchronisation classifier for fingerprint identification," *IET Image Process.*, vol. 8, no. 6, pp. 354–362, Jun. 2014.
[26] C. Chi and F. Gao, "Palm print edge extraction using fractional differential algorithm," *J. Appl. Math.*, vol. 2014, pp. 1–7, Apr. 2014.
[27] S. M. Bhandarkar, Y. Zhang, and W. D. Potter, "An edge detection technique using genetic algorithm-based optimization," *Pattern Recognit.*, vol. 27, no. 9, pp. 1159–1180, Sep. 1994.
[28] R. M. Naife and H. H. Abass, "Optimal edge detection filter using genetic algorithm," *J. Kerbala Univ.*, vol. 13, no. 1, pp. 149–160, 2015.
[29] M. A. Awal and B. Boashash, "An automatic fast optimization of quadratic time-frequency distribution using the hybrid genetic algorithm," *Signal Process.*, vol. 131, pp. 134–142, Feb. 2017.
[30] J. M. M. C. Adhikary, "Medical image edge detection based on soft computing approach," *Int. J. Innov. Res. Comput. Commun. Eng.*, vol. 3, no. 7, pp. 6801–6807, Aug. 2015.
[31] N. S. Joshi and N. Choubey, "Application of soft computing approach for edge detection," *Int. J. Appl. Innov. Eng. Manage.*, vol. 3, no. 4, pp. 116–122, 2014.
[32] W. El-Araby, A. Madian, M. Ashour, I. Farag, and M. Nassef, "Radiographic images fractional edge detection based on genetic algorithm," *Int. J. Intell. Eng. Syst.*, vol. 11, pp. 158–166, Aug. 2018.
[33] L. Cadena, N. Espinosa, F. Cadena, A. Korneeva, A. Kruglyakov, A. Legalov, A. Romanenko, and A. Zotin, "Brain's tumor image processing using shearlet transform," *Proc. SPIE*, vol. 10396, Sep. 2017, Art. no. 103961B.
[34] S. Vaishali, K. K. Rao, and G. V. S. Rao, "A review on noise reduction methods for brain MRI images," in *Proc. Int. Conf. Signal Process. Commun. Eng. Syst.*, Jan. 2015, pp. 363–365.
[35] M. Mafi, H. Martin, M. Cabrerizo, J. Andrian, A. Barreto, and M. Adjouadi, "A comprehensive survey on impulse and Gaussian denoising filters for digital images," *Signal Process.*, vol. 157, pp. 236–260, Apr. 2019.
[36] L. Qiusheng, F. Xiaoyu, S. Baoshun, and Z. Xiaohua, "Compressed sensing MRI based on the hybrid regularization by denoising and the epigraph projection," *Signal Process.*, vol. 170, May 2020, Art. no. 107444.
[37] O. Li and P.-L. Shui, "Subpixel blob localization and shape estimation by gradient search in parameter space of anisotropic Gaussian kernels," *Signal Process.*, vol. 171, Jun. 2020, Art. no. 107495.
[38] G. Liu and M. Deng, "Parametric active contour based on sparse decomposition for multi-objects extraction," *Signal Process.*, vol. 148, pp. 314–321, Jul. 2018.
[39] M. Li, L. Kuang, S. Xu, and Z. Sha, "Brain tumor detection based on multimodal information fusion and convolutional neural network," *IEEE Access*, vol. 7, pp. 180134–180146, 2019.
[40] W. Dou, S. Ruan, Y. Chen, D. Bloyet, and J.-M. Constans, "A framework of fuzzy information fusion for the segmentation of brain tumor tissues on MR images," *Image Vis. Comput.*, vol. 25, no. 2, pp. 164–171, Feb. 2007.
[41] G. Moonis, J. Liu, J. K. Udupa, and D. B. Hackney, "Estimation of tumor volume with fuzzy-connectedness segmentation of MR images," *Amer. J. Neuroradiol.*, vol. 23, no. 3, pp. 356–363, 2002.
[42] M. BachCuadra, C. Pollo, A. Bardera, O. Cuisenaire, J.-G. Villemure, and J.-P. Thiran, "Atlas-based segmentation of pathological MR brain images using a model of lesion growth," *IEEE Trans. Med. Imag.*, vol. 23, no. 10, pp. 1301–1314, Oct. 2004.
[43] J. J. Corso, E. Sharon, and A. Yuille, "Multilevel segmentation and integrated Bayesian model classification with an application to brain tumor segmentation," in *Proc. Int. Conf. Med. Image Comput. Comput.-Assist. Intervent.* Berlin, Germany: Springer, 2006, pp. 790–798.

[44] P. Sharma, M. Diwakar, and S. Choudhary, "Application of edge detection for brain tumor detection," *Int. J. Comput. Appl.*, vol. 58, no. 16, pp. 21–25, Nov. 2012.
[45] A. Bhide, P. Patil, and S. Dhande, "Brain segmentation using fuzzy C means clustering to detect tumour region," *Int. J. Adv. Res. Comput. Sci. Electron. Eng.*, vol. 1, no. 2, pp. 85–90, 2012.
[46] Z. Stosic and P. Rutesic, "An improved canny edge detection algorithm for detecting brain tumors in MRI images," *Int. J. Signal Process.*, vol. 3, pp. 1–5, Mar. 2018.
[47] Priya and V. S. Verma, "New morphological technique for medical image segmentation," in *Proc. 3rd Int. Conf. Comput. Intell. Commun. Technol. (CICT)*, Feb. 2017, pp. 1–5.
[48] R. C. Patil and A. Bhalchandra, "Brain tumour extraction from MRI images using MATLAB," *Int. J. Electron., Commun. Soft Comput. Sci. Eng.*, vol. 2, no. 1, pp. 1–4, 2012.
[49] J. H. Holland, *Adaptation in Natural and Artificial Systems: An Introductory Analysis With Applications to Biology, Control, and Artificial Intelligence*. Cambridge, MA, USA: MIT Press, 1992.
[50] A. Meyer-Baese and V. J. Schmid, *Pattern Recognition and Signal Analysis in Medical Imaging*. Amsterdam, The Netherlands: Elsevier, 2014.
[51] D. Whitley, "A genetic algorithm tutorial," *Statist. Comput.*, vol. 4, no. 2, pp. 65–85, 1994.
[52] Z. Michalewicz, "Genetic algorithms, numerical optimization, and constraints," in *Proc. 6th Int. Conf. Genet. Algorithms*, vol. 195, 1995, pp. 151–158.
[53] T. J. Keating, P. Wolf, and F. Scarpace, "An improved method of digital image correlation," *Photogramm. Eng. Remote Sens.*, vol. 41, no. 8, pp. 993–1002, 1975.
[54] Z. Wang, A. C. Bovik, H. R. Sheikh, and E. P. Simoncelli, "Image quality assessment: From error visibility to structural similarity," *IEEE Trans. Image Process.*, vol. 13, no. 4, pp. 600–612, Apr. 2004.
[55] I. E. Abdou and W. K. Pratt, "Quantitative design and evaluation of enhancement/thresholding edge detectors," *Proc. IEEE*, vol. 67, no. 5, pp. 753–763, May 1979.
[56] A. Carass, J. Cuzzocreo, M. B. Wheeler, P.-L. Bazin, S. M. Resnick, and J. L. Prince, "Simple paradigm for extra-cerebral tissue removal: Algorithm and analysis," *NeuroImage*, vol. 56, no. 4, pp. 1982–1992, Jun. 2011.
[57] L. J. Guo, "Balance contrast enhancement technique and its application in image colour composition," *Int. J. Remote Sens.*, vol. 12, no. 10, pp. 2133–2151, Oct. 1991.
[58] K. Clark, B. Vendt, K. Smith, J. Freymann, J. Kirby, P. Koppel, S. Moore, S. Phillips, D. Maffitt, M. Pringle, L. Tarbox, and F. Prior, "The cancer imaging archive (TCIA): Maintaining and operating a public information repository," *J. Digit. Imag.*, vol. 26, no. 6, pp. 1045–1057, Dec. 2013.

AHMED H. ABDEL-GAWAD was born in 1994. He received the B.Sc. degree (Hons.) in communication and electronics engineering, in 2018. He is currently pursuing the M.Sc. degree in microelectronics system design (MSD) with the Nanoelectronics Integrated System Center (NISC), Nile University, Giza. He has been a Teaching Assistant with the School of Engineering and Applied Sciences, Nile University, since 2018. He won the first place on TIEC's graduation projects competition (IBTIECAR 2018), communications track.

LOBNA A. SAID (Senior Member, IEEE) received the B.Sc., M.Sc., and Ph.D. degrees in electronics and communications from Cairo University, Egypt, in 2007, 2011, and 2016, respectively.

She is currently a full-time Assistant Professor with the Nano-Electronics Integrated System Research Center (NISC), Faculty of Engineering and Applied Science, Nile University (NU). She has over 86 publications distributed between high-impact journals, conferences, and book chapters. She was involved in many research grants as a Senior Researcher, or as a Co-PI from different national organizations. Her research interests include interdisciplinary, including system modeling, control techniques, optimization techniques, analog and digital integrated circuits, fractional-order circuits and systems, nonlinear analysis, and chaos theory. She was selected as a member of the Egyptian Young Academy of Sciences (EYAS) to empower and encourage young Egyptian scientists in science and technology and build knowledge-based societies. In 2020, she was selected to be an Affiliate Member of the African Academy of Science (AAS). She has received the Recognized Reviewer Award from many international journals. She has received the Excellence Award from the Center for the Development of Higher Education and Research, in 2016. She is the Winner of Dr. Hazem Ezzat Prize for the Outstanding Researcher, NU, in 2019. She is one of the top ten researchers at NU, for the year 2018–2019. She is the Vice-Chair of research activities at the IEEE Computational Intelligence Egypt Chapter. She is also in the Technical Program Committee for many International Conferences.

AHMED G. RADWAN (Senior Member, IEEE) was the Former Director of the Nanoelectronics Integrated Systems Center (NISC), Nile University, Egypt. He was the Former Director of the Technical Center for Carrier Development (TCCD), Cairo University, Egypt. He is currently the Vice President for Research with Nile University and a Professor with the Department of Engineering Mathematics and Physics, Cairo University. He has more than 300 papers, and more than 5000 citations based on Scopus database, seven international books, and 18 book chapters in the highly ranked publishers, such as Elsevier and Springer. He has six U.S. patents in several topics. His research interests include interdisciplinary concepts between mathematics and engineering applications, such as fractional-order systems, bifurcation, chaos, memristor, and encryption.

Prof. Radwan is a member of the National Committee of Mathematics and the Applied Science Research Council, specialized scientific councils, Academy of Scientific Research and Technology (ASRT), Egypt. He was a Former Member of the Egyptian Young Academy of Science (EYAS), ASRT. He was selected as a MC Observer to COST Action CA15225. During the last ten years, he has many academic visits as the Session Chair/Organizer, an Invited Speaker, and attending international conferences in several countries. Based on Scival database, he is one of the top authors worldwide for the two research tracks Capacitors—Networks (circuits)—Fractional-order capacitor (T.21555) and Chaos theory—Chaotic systems—Multi-scroll chaotic (T.8806). He received the State Achievements Award for research in mathematical sciences, in 2012, the Cairo University Achievements Award for research in the engineering sciences, in 2013, the Abdul Hameed Shoman Award for Arab researchers in basic sciences (Information and Data Security), in 2015, the Best Researcher Awards Nile University, in 2015 and 2016, the Cairo University Excellence Award for research in the engineering sciences, in 2016, the Prof. Mohamed Amin Lotfy Award from ASRT in the mathematical sciences, in 2016, the Scopus Award in engineering and technology from Elsevier, in 2019, as the Top Researcher in Egypt, from 2014 to 2018, (based on H-index, field-weighted citation impact, and number of publications), the State First-Class Medal of Science and Arts, and the State Excellence Award in advanced technological sciences, in 2018. He has honored from Cairo University President in the 13th and 15th Cairo University Science Festival Days, in December 2015 and 2017, respectively. He is the Founder and the General Co-Chair of the 1st and 2nd Novel Intelligent and Leading Emerging Sciences conference NILES2019NILES2020, Egypt. He was the Technical Program Co-Chair of many international conferences. He is selected in the editorial board of the *Journal of Engineering and Applied Science* and the Lead/Guest Editor of different special issues in many high-valued journals.